Prospect for Experimental Investigation of Phase-Space Turbulence in Magnetically Confined Fusion Plasmas*)

Tatsuya KOBAYASHI[1,2)]

[1)]*National Institute for Fusion Science, National Institutes of Natural Sciences, Toki 509-5292, Japan*
[2)]*The Graduate University for Advanced Studies, SOKENDAI, Toki 509-5292, Japan*

(Received 7 December 2022 / Accepted 14 June 2023)

In this paper the prospect of experimental investigation of phase-space turbulence in magnetically confined fusion plasmas is assessed, motivated by a theoretical suggestion of its potential role in turbulent anomalous transport conundrums. Three experimental approaches regarding (i) fusion plasma experiment, (ii) basic plasma experiment, and (iii) simulation data analysis are considered, accounting for challenges and expected outcomes. Platforms for experiments ranging from high-temperature fusion plasmas to low-temperature linear plasmas, are overviewed. Interdisciplinary interests regarding phase-space turbulence in magnetosphere plasmas and laser wake-field acceleration are also discussed.

Keywords: phase-space turbulence, turbulent transport, electron helo, fusion plasma, magnetosphere plasma, laser wake-field accerelation

DOI: 10.1585/pfr.18.2402059

1. Introduction

In magnetically confined plasma fusion development, one of the greatest problems for successfully acquiring a commercial reactor is the power degradation problem. When increasing heating power aiming at achieving high temperature in core plasma, the plasma confinement time degrades accordingly. This feature is clearly seen in the confinement time scaling as,

$$\tau_E^{\mathrm{scale}} \propto P^{\alpha_P}, \tag{1}$$

where P is the plasma heating power and exponent α_P typically takes a negative value around ~ -0.5 in a wide parameter range and in different devices with a large diversity in plasma size [1,2]. This feature also holds regardless of magnetic field configuration, i.e., both in tokamaks and stellarators/heliotrons. Because of the power degradation problem, achieving the Lawson criterion is a great challenge. Thanks to the continuous efforts of researchers at uncovering the background physics of the power degradation problem, it has been found that turbulence plays the decisive role in anomalous transport under a high heating power application [3].

In order to describe turbulent transport properties, quasilinear model was established. In the quasilinear model, the transport flux of any physical quantity of interest Ψ is approximated as

$$\Gamma_r \equiv \langle \tilde{v}_r \tilde{\Psi} \rangle \sim -D \partial \langle \Psi \rangle / \partial r, \tag{2}$$

where Γ_r is the radial (cross-field) transport flux, v_r is the radial velocity, $\langle\rangle$ is the long time average, and the tilde denotes fluctuation quantities [4–6]. In the quasilinear model, the diffusion coefficient is given as $D \sim \gamma/k^2$, where γ and k show the linear growth rate and the wavenumber of turbulence. Due to its convenience, the quasilinear model is applied in experimental analyses. For instance, an experimental determination of D [7] and scaling analysis [8], direct observation of turbulence behavior [9], and gyrokinetic simulation for speculating the physics behind it [10], have been performed. Thanks to those efforts, qualitative and occasionally quantitative understandings of turbulent transport were obtained, which were also applied to performance projection for future devices such as ITER and DEMO [11].

However, there are still several observations that cannot be explained by the quasilinear model. Those are, for example, nondiffusive transport [12,13], nonlocal/transient transport [14, 15], profile stiffness [16, 17], and others. Those transport events are called the transport conundrums in this paper. As a specific example in the W7-AS stellarator, the experimentally determined diffusion coefficient surges immediately after applying an additional electron cyclotron resonance heating (ECRH), although local parameters largely do not change [18]. Since the quasilinear model manifests that the transport coefficient must be a function of the local parameters and their gradient, this observation is considered to be a clear counterexample to the quasilinear model. Analogous observations were also reported in different devices, such as TFR [19], DIII-D [20], and LHD [21]. The transport conundrums may not be accounted for only by extending the quasilinear model. Another framework is necessary.

Phase-space turbulence is a potential candidate for a

author's e-mail: kobayashi.tatsuya@nifs.ac.jp

*) This article is based on the presentation at the 31st International Toki Conference on Plasma and Fusion Research (ITC31).

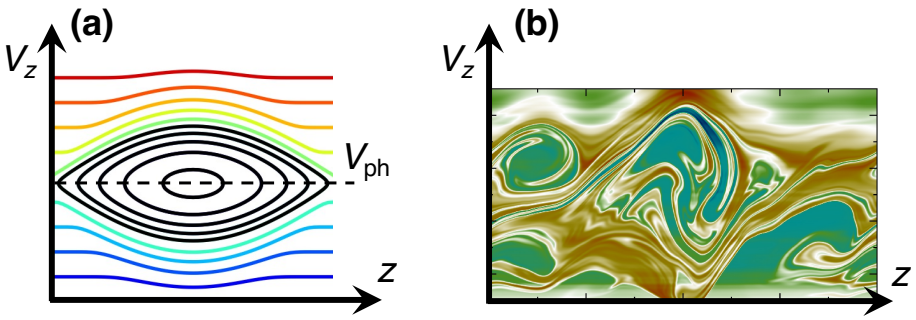

Fig. 1 (a) Illustration of phase-space Bernstein Greene Kruskal (BGK) vortex and (b) snapshot of phase-space turbulence in a kinetic simulation, reproduced from [22], with the permission of AIP Publishing. V_{ph} is the phase velocity of wave.

model that can account for the transport conundrums [23]. In high-temperature plasmas, particle collision frequencies that are inversely proportional to the temperature to the power of 1.5, are generally low. When the particle collision time τ_{coll}, the wave correlation time τ_{corre}, and the bounce time of particles trapped in the wave τ_{bounce} are in the following relation; $\tau_{coll} > \tau_{corre} > \tau_{bounce}$, nonlinear mutual interaction between the wave and particles becomes meaningful. For example, a local deficit of particles enhancing the potential wave depth is called the electron hole [24]. This structure of the wave and particles can be persistent enough to impact on plasma transport in high-temperature and low-collision plasmas. The trajectories of trapped particles drawn in the phase-space, i.e., a plane spanned by the real-coordinate and the velocity-coordinate, form a vortex-like structure, as shown in Fig. 1 (a). This structure is called the Bernstein Greene Kruskal (BGK) vortex [25]. The BGK vortex is centered at the phase velocity of the wave V_{ph} in the velocity-coordinate. In magnetically confined plasmas, the BGK vortex eventually evolves into a turbulent state [26], as shown in Fig. 1 (b) [22].

The phase-space structure formation is a nonlinear phenomenon. The wave-particle nonlinear interaction is described in the Vlasov-Poisson system, i.e.,

$$\frac{\partial f}{\partial t} + v\frac{\partial f}{\partial x} - \frac{q}{m}\frac{\partial \phi}{\partial x}\frac{\partial f}{\partial v} = 0, \tag{3}$$

$$-\epsilon_0 \frac{\partial^2 \phi}{\partial x^2} = n_0 \sum_i q_i \int dv f_i, \tag{4}$$

where f is the velocity distribution function, m and q are the mass and charge of the particle of interest, respectively, ϕ is the electrostatic potential, n_0 is the equilibrium plasma density, and ϵ_0 is the permittivity of the vacuum. For Eq. (4), the summation is taken for trapped and passing particles of the same charge, and opposingly charged particles [27]. Note that taking only the real-space perturbation and neglecting nonlinearity, the conventional fluid approach providing, e.g., the Langmuir wave, recovers. Nonlinearity appears predominantly in the second and third terms of Eq. (3). The actual form of the phase-space structure can be derived as one that maximizes entropy that is directly defined by the velocity distribution function [24].

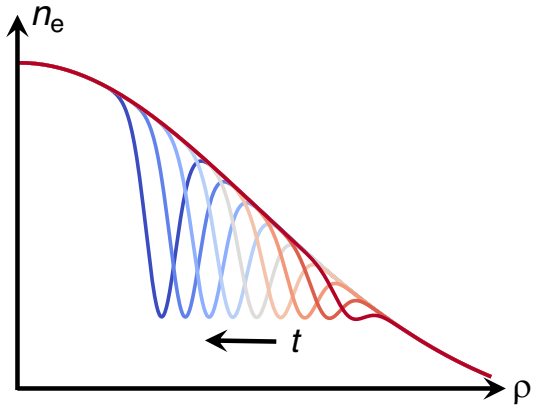

Fig. 2 Growth of an electron hole on density profile having real-space gradient.

In theoretical works, the outcomes of phase-space turbulence on transport are predicted. For example, the convection transport term emerges in addition to the diffusion term [23, 28]. The phase-space structure can form on a faster time scale than the real-space profile evolution, therefore the phase-space turbulence can induce non-local/transient transport [29, 30]. In the marginal stability condition for a fluid turbulence, i.e., the profile saturation state, the quasilinear theory predicts zero transport flux, although continuous energy input to the system is applied to maintain the nonequilibrium system. In such a case, transport flux induced by the phase-space turbulence dominates the total flux and impacts on the "stiff" profile determination [31, 32]. Moreover, the phase-space turbulence can release free energy from the real-space gradient. For example, the phase-space electron hole can have an up-gradient transportation, as shown in Fig. 2, by which the depth of the structure grows [27]. The growth rate of the structure is predicted to be amplitude dependent, therefore, an explosive growth (faster than linear growth) is possible [33]. All of those can be possible solutions for transport conundrums [23]. Nevertheless, due to experimental difficulty, direct observation of phase-space turbulence and investigation into the role of phase-space turbulence on transport have not been done.

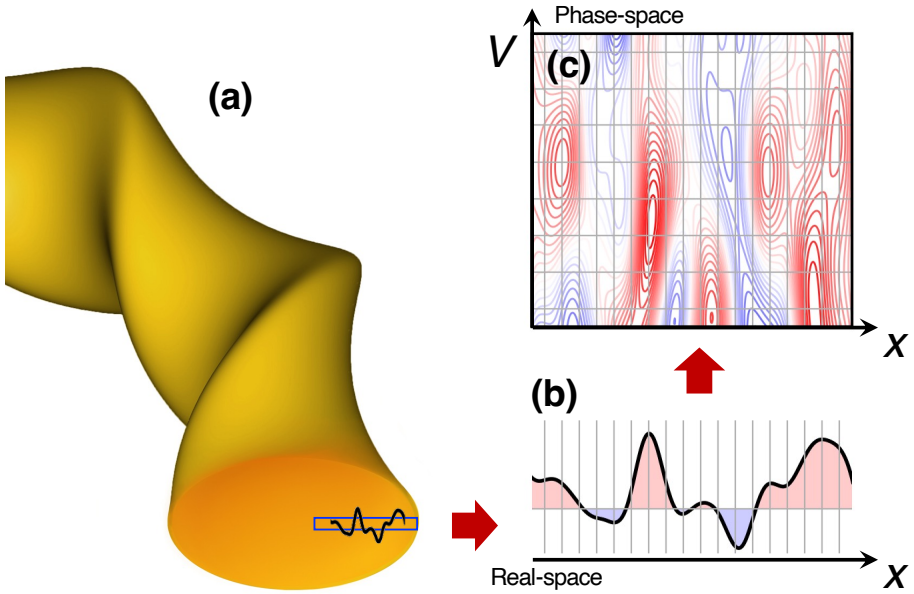

Fig. 3 (a) Schematic of the fluctuation measurement with (b) real-space sampling and (c) phase-space sampling.

2. Experimental Perspective

To reveal the physics background of the transport conundrums, experimental study having a kinetic viewpoint of plasma turbulence is required. However, phase-space decomposed fluctuation diagnostics, which are key ingredients of experimental study, are still challenging. Let us consider the situation in Fig. 3. In a real-space fluctuation measurement, a space of interest is sampled with a specific resolution, as shown in Fig. 3 (b). The signal intensity in each sampling bin is normally diagnosed by a detector array. For phase-space decomposition, however, the signal intensity in the sampling bin must be further extended into the velocity-space coordinate in, for example, a spectroscopic manner. This generally makes the signal intensity, in a single sampling bin, on the phase-space much smaller. In other words, a trade-off among the signal intensity and sampling resolutions in real-space, velocity-space, and time must be accounted for. It is also difficult to find a multidimensional detector array with a fast operation capability. Another challenge is the limitation of diagnostic principles. For example, the Heterodyne interferometer, which is a prevalent plasma density diagnostic principle, cannot be directly extended in velocity-space measurement. Nevertheless, the recent remarkable development of diagnostic systems is expanding research opportunities. In this paper, three aspects of possible experimental approaches regarding (i) fusion plasma experiment, (ii) basic plasma experiment, and (iii) simulation data analysis are featured.

2.1 Fusion plasma experiment

In fusion plasma experiment, direct or indirect measurement of phase-space structures is the main objective, by which transport physics is considered and conundrums are discussed. For this purpose, development of state-of-the-art phase-space diagnostic systems is necessary. At the same time, operation of conventional diagnostic systems with problem-specific optimizations is also essential. In this subsection, an overview of recent remarkable results in Large Helical Device (LHD) is presented as an example of research activity.

In LHD, a two-dimensional optical fiber array is installed in the vertical and radial directions for versatile optical measurement purposes, which is shown by grey symbols in Fig. 4 (a). In the conventional CXS system, 36 channels of radially aligned fibers are used for the profile measurement of the carbon impurity ion distribution function. A result of the measurement, the carbon ion temperature that is considered to reflect the main ion temperature, is shown in Fig. 4 (b). Although the profile measurement is reasonably performed, the conventional system is not applicable for measurement of velocity-space structures with a short lifetime.

For instance, there was an attempt to measure an energetic particle-driven magnetohydrodynamic (MHD) burst [34, 35] by the conventional CXS system, as shown in Fig. 5 (b). The time scale of events is around 2 - 3 ms (Fig. 5 (a)), which is shorter than the time resolution of the conventional CXS system of 5 ms. In order to improve the time resolution, the exposure time of the charge coupled device (CCD) detector must be shortened, which results in a low signal intensity accordingly. To realize the fast measurement, the lost signal intensity must be compensated for. In the new system, fifty fibers are binned for one detector channel, which instead degrades the spatial resolution. This also limits the maximum available channel number up to four (in this case three) so profile measurement is not possible. Nevertheless, a time resolution of

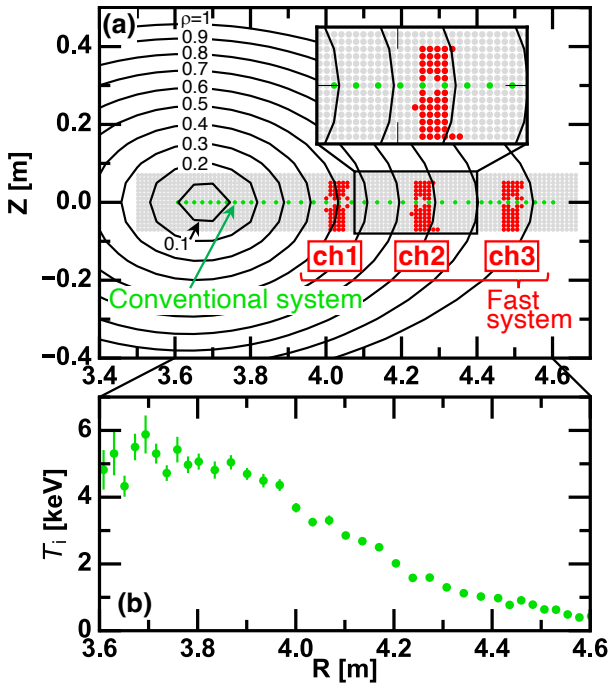

Fig. 4 (a) Lines of sight for the charge exchange recombination spectroscopy (CXS) system on the LHD poloidal cross section and (b) ion temperature profile obtained by conventional CXS system.

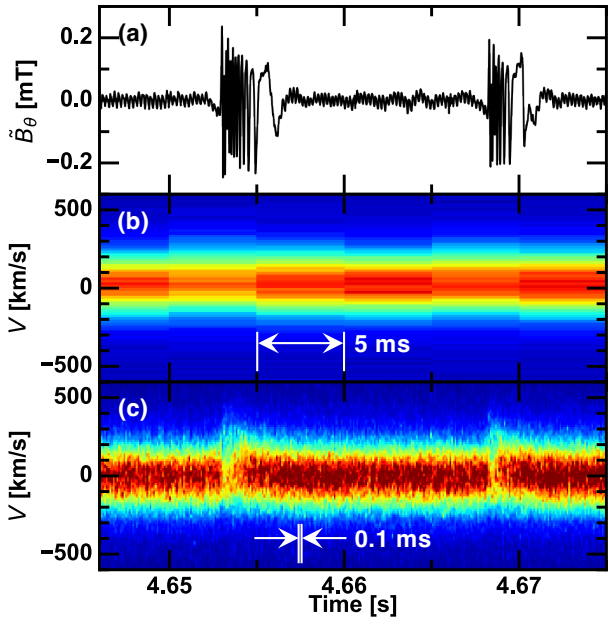

Fig. 5 Time evolutions of (a) poloidal magnetic field fluctuation, velocity distribution functions measured by (b) conventional CXS and (c) fast CXS across which MHD burst events emerge. (Shot number: 171957)

0.1 ms is achieved as shown in Fig. 5 (c). Thanks to this improvement, the distribution function deformation induced by MHD burst events is successfully measured [36].

Results of the measurement are shown in Fig. 6. Velocity distribution functions, f, before and after a MHD

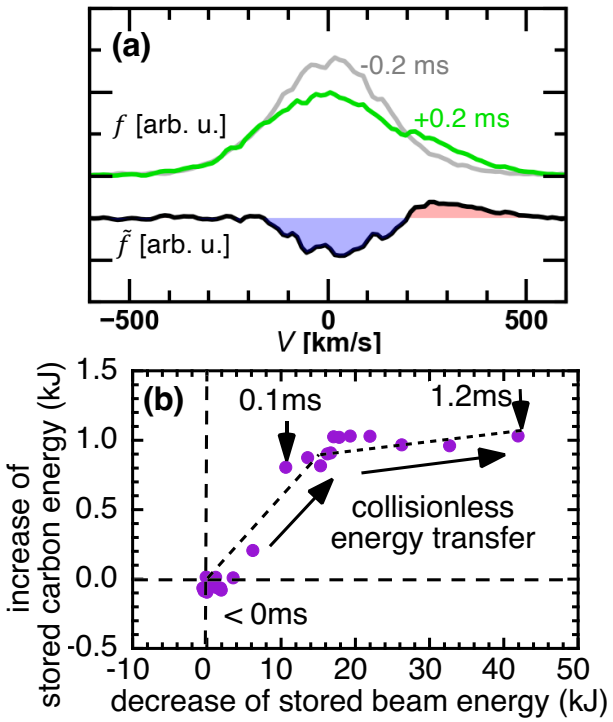

Fig. 6 (a) Velocity distribution functions, f, before and after MHD burst event obtained with conditional average and their difference, $\tilde{f}$, and (b) comparison between increase in carbon stored energy and decrease in beam stored energy. Reproduced from [36] under a CC BY 4.0 license (https://creativecommons.org/licenses/by/4.0/). Created by modifying original figures.

burst event are obtained by an event-wise conditional average for ruling out unreproducible parts. Their difference, $\tilde{f}$, is also shown, where the energy lost and gained are depicted by blue and red shades, respectively. The observed asymmetric dipole structure is a signature of the nonlinear Landau damping induced by the MHD burst event. Note that the total energy gain of carbon ions across the event is approximately 25 % of the thermal energy, which is considerable. By comparing the increase in carbon stored energy and decrease in beam stored energy, nonlinear energy transfer from beam to plasma, mediated by a wave, is discussed. Here, the beam stored energy is evaluated from the neutron flux diagnostics. In this example, the MHD burst event is known to have a low order toroidal mode number of $n = 1$ according to magnetic fluctuation measurement. In this case, the spatial integration with fifty fibers is allowed mostly without losing observation rigor. Such a physics target-specific diagnostic optimization is essential to reasonably detect a phase-space structure under the trade-off constraint, as discussed above. Recently, a new tomographic approach has been proposed for reconstructing the phase-space structure, based on different kinds of integration data in real-space, velocity-space, and time [37]. With those hardware and software techniques for phase-space structure detection, potential physics targets at the first step are the MHD driven events, global

or mesoscale structures, and externally driven transport events, which have relatively slow time scales and large spatial scales.

2.2 Basic plasma experiment

Nonetheless, direct detection of smaller scale phase-space structures in high-temperature fusion plasmas is still challenging. In order to investigate the fundamental physics of phase-space turbulence, use of basic plasma devices is an attractive option. In particular, there are well-established active excitation techniques for the phase-space structures, such as electrode biassing [38], electron beam [39], magnetic reconnection [40], and others. Thanks to the low temperature of target plasmas, direct use of electrostatic probes is allowed, which have high sensitivity [39]. A famous example is shown in Fig. 7 as an instance, where a linear device having an electrostatic bias exciter was used for actively driving phase-space electron holes [38]. Formed structures were detected by the electrostatic probes. It should be noted that the sign of the measured potential ϕ (bottom six plots in Fig. 7) is inverted in the figure. The positive potential pulse corresponds to the local deficit of electrons on a velocity range close to the wave propagation velocity on the magnetic field direction. As the experiment is performed on a one-dimensional column, a cross-field vortex structure predicted in [27] may not be formed. In a numerical simulation for interpreting this experiment, a hole structure on the electron velocity distribution function is found. Note that the signal intensity is remarkably high even with the sub-microsecond time scale. By utilizing such kinds of devices, it is essential to attempt to resolve the velocity-space structure in addition to the real-space structure, likely by changing probe biasing voltage. Since the probe biasing voltage is generally changed in a voltage sweeping manner, time resolution, velocity-space resolution, and signal intensity are in a trade-off relation. Direct measurement of the phase-space BGK hole, which eventually evolves into a turbulent state, would be a main objective of the basic experiment. Scaling study of hole characteristics, such as the propagation velocity and the lifetime, on plasma parameters is essential for projecting phase-space structure properties in fusion plasmas. Moreover, how it couples with the real-space gradient (see Fig. 2) and how transport differs from that induced by fluid turbulence are of great interest in the context of the magnetically confined fusion plasma study.

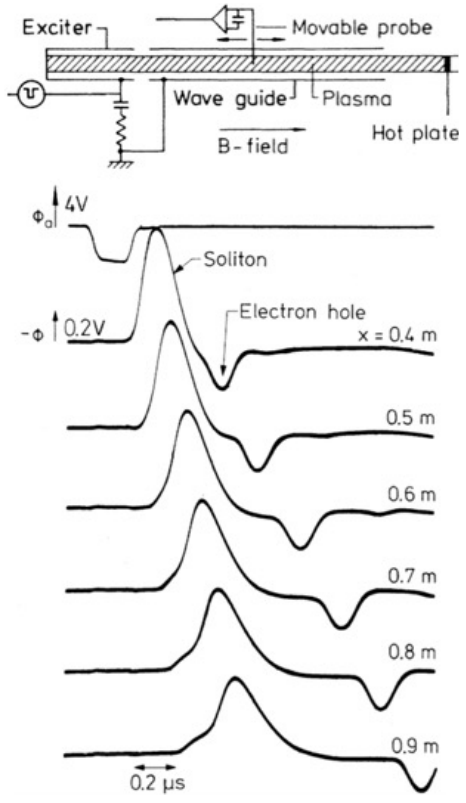

Fig. 7 Schematic view of basic plasma experiment: (top) a linear device having an electrostatic bias exciter used for actively driving phase-space electron holes and then (bottom) formed structures detected by electrostatic probes [38]. It should be noted that the sign of measured potential ϕ (bottom six plots) is inverted in the figure. Copyright (1979) by the American Physical Society.

2.3 Simulation data analysis

Due to the limited opportunity for experimental study of phase-space turbulence, the aid of kinetic simulation works is inevitable. Recently, a direct survey of phase-space structures in kinetic simulation data was performed [41]. Figure 8 (a) shows the perturbed part of the phase-space structure in a set of fixed positions except for the toroidal angle and the parallel velocity coordinates during an avalanche event. Here, the avalanche event refers to the nonlocal propagation of turbulence clump in the radial direction. Toroidally dependent and positive-negative parallel velocity asymmetric phase-space structures were found, which were characteristic features in this phase and were qualitatively different from those in the quiescent phase. Since the simulation results in five-dimensional space were far too tangled to analyze and even to visualize, the principal component analysis was applied, aiming at dimension reduction and interpretation. Using this method, a large part of the 6 dimensional data was successfully described in a limited number of degrees of freedom, and characteristic properties of the phase-space structures accompanied by the avalanche event was uncovered.

A turbulence diagnostic simulator in an actual experimental setup (e.g., Fig. 8 (b)) is another promising numerical tool for searching for "footprints" of phase-space turbulence on conventional real-space turbulence diagnostics [42]. In this study, the expected diagnostic data was inferred using a gyrokinetic simulation code by mimicking the diagnostic principle in the actual geometry for examining the diagnostic resolution and interpreting obtained data. Here, the simulated phase-space structure was

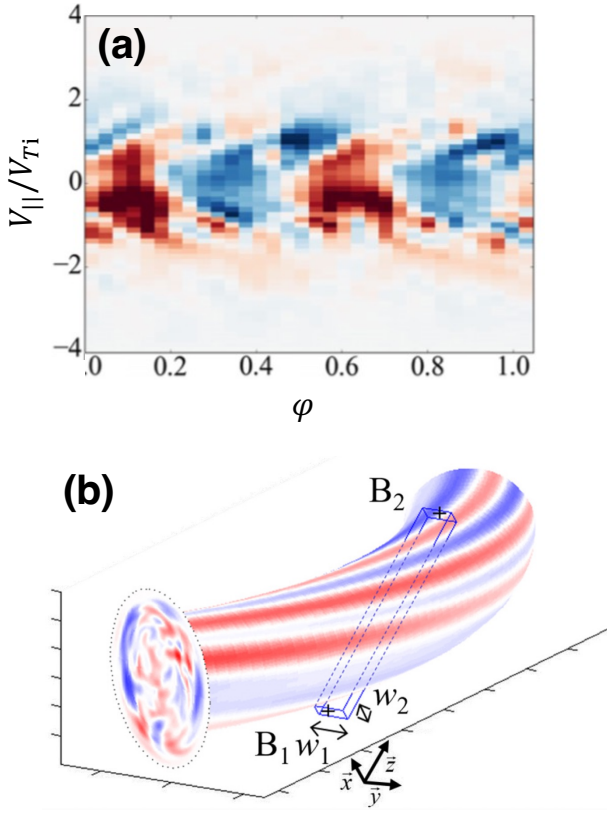

Fig. 8 (a) Survey of phase-space structure in five-dimensional kinetic simulation space, reproduced from [41], with the permission of AIP Publishing, and (b) numerical turbulence diagnostic simulator [42].

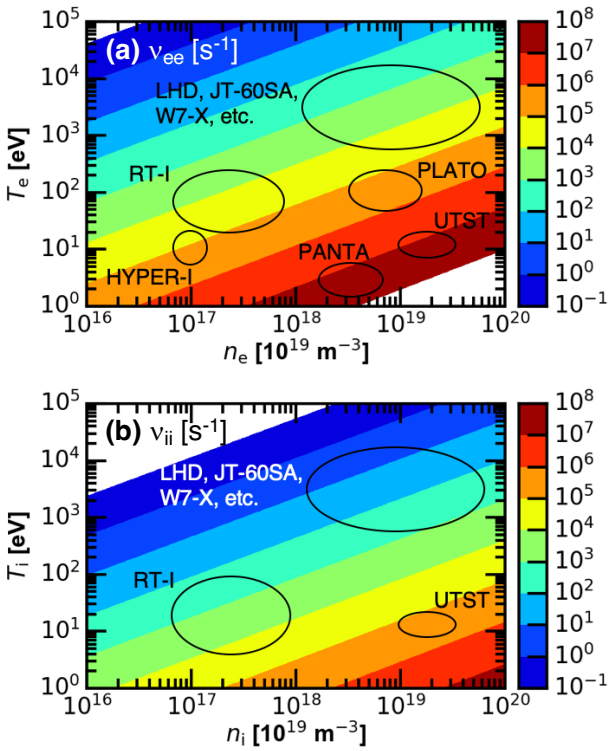

Fig. 9 Collision frequencies between (a) electrons and (b) ions plotted with parameter coverage of different kinds of potential experimental platforms for phase-space turbulence study.

not explicitly treated since the target turbulence diagnostic was real-space based. However, in future, it will be possible to extend this activity towards phase-space diagnostics such as the charge exchange recombination spectroscopy for interpreting measured data and improving diagnostic performance. Diagnostic simulation is also essential for physics target-specific diagnostic optimization, as mentioned above. A full-f global gyro-kinetic simulation code would be a powerful tool for making those simulations [43].

3. Potential Platforms

As was discussed above, different varieties of experimental platforms are potentially used for phase-space turbulence study. Here, the prospect of a measurement opportunity is assessed in terms of the time resolution. Figures 9 (a) and (b) show the electron-electron and ion-ion collision frequencies, respectively, on which parameter coverage of different kinds of potential experimental platforms is displayed. The diagnostic system must have a higher time resolution at least than the collision frequency, below which the trajectory of particles trapped by a wave is no longer maintained. Platform candidates, collision frequencies, and potential diagnostics are summarized in Table 1. In fusion and dipole devices, due to relatively low collision frequencies, operation of spectroscopy and microwave diagnostics is allowed for the phase-space structure measurement. In LHD, a Thomson scattering system equipped with high intensity lasers was recently upgraded to have a high repetition rate of $O(10^4)$ s^{-1}, which was potentially available for obtaining information about the electron velocity distribution function [44]. In basic devices, due to relatively low plasma temperature, the collision frequency is high. However, electrostatic probes can be used, which has high sensitivity and therefore fine time resolution.

4. Interdisciplinary Interest

Phase-space turbulence or wave-particle nonlinear interaction is a ubiquitous phenomenon in any low collision plasmas. There are interdisciplinary interests regarding the nonlinear process of structure formation and outcomes of wave-particle interaction, e.g., particle acceleration and transport. In magnetosphere plasmas, electron hole evolution is actively studied, both by using satellites [46] and laboratory plasma devices [47]. There, collisionless energy exchange between waves and particles is one of the central interests [48]. In laser wake-field acceleration [49], bunching of plasma and steepening of the wave field are observed in its nonlinear phase (Fig. 10) [45]. This feature contrasts with the case of magnetically confined plasmas, where

Table 1 List of experimental platforms and potentially used diagnostics.

Category	Devices	ν_{ee} [s^{-1}]	ν_{ii} [s^{-1}]	Diagnostics
Fusion	LHD, JT-60SA	10^{4-6}	10^{1-3}	Spectroscopy, microwave, laser
Dipole	RT-I	10^{4-6}	10^{3-5}	Spectroscopy, microwave, probe
Basic torus	UTST, PLATO	10^{6-8}	10^{5-6}	Probe
Linear	PANTA, HYPER-I	10^{5-8}	–	Probe

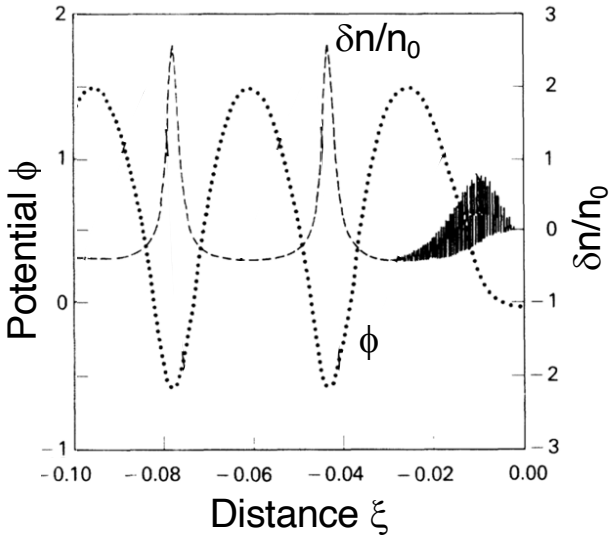

Fig. 10 Traveling potential wave and plasma density perturbation in laser wake-field acceleration [45]. Copyright (1990) by the American Physical Society.

phase-space turbulence is predicted to evolve, as shown in Fig. 1 (b). Finding a case dependent selection rule of the nonlinear process is an interesting academic challenge. As noted above, the phase-space structure is predicted to have a state that maximizes the entropy directly defined by the velocity distribution function. Direct measurement of the velocity distribution function can therefore contribute to an examination of the dissipative structure formation theorem in an open nonequilibrium system.

5. Summary

According to the theoretical suggestion of important roles of phase-space turbulence on unresolved turbulent transport properties in magnetically confined plasmas, the prospect of experimental investigation of turbulence in phase-space was assessed. Three experimental approaches regarding (i) fusion plasma experiment, (ii) basic plasma experiment, and (iii) simulation data analysis, were overviewed, each of which had challenges, and expected outcomes were discussed. Experimental platforms ranging from high-temperature fusion plasmas to low-temperature linear plasmas were outlined. Interdisciplinary interests regarding the phase-space turbulence in magnetosphere plasmas and laser wake-field acceleration were also discussed.

Acknowledgments

The author acknowledges Drs. K. Ida, Y. Kawachi, N. Kenmochi, N. Tamura, T. Tokuzawa, M. Nishiura, R. Yanai, I. Yamada, M. Yoshinuma, T. Ido, M. Inomoto, M. Okamura, S. Kubo, H. Saito, M. Sasaki, N. Sato, Y. Tatematsu, T. Ii Tsujimura, Y. Nagashima, S. Nishimura, R. Numata, M. Fukunari, and A. Fujisawa for useful discussion. Also, Drs. A. Ando, K. Itoh, M. Kikuchi, Y. Kishimoto, Y. Kimura, A. Sagara, T. Sato, H. Takabe, M. Toriumi, A. Hasegawa, K. Mima, H. Yamada, and Z. Yoshida are acknowledged for their support and encouragement. The author also thanks Drs. M. Lesur, M. Kando, and Y. Kosuga for their help. This work is partly supported by the Grant-in-Aid for Scientific Research of JSPS (21H04973 and 21K13902).

Data availability

The LHD data can be accessed from the LHD data repository (www-lhd.nifs.ac.jp/pub/Repository_en.html).

[1] P.N. Yushmanov, T. Takizuka, K.S. Riedel, O.J.W.F. Kardaun, J.G. Cordey, S.M. Kaye and D.E. Post, Nucl. Fusion **30**, 1999 (1990).
[2] H. Yamada, J.H. Harris, A. Dinklage, E. Ascasibar, F. Sano, S. Okamura, J. Talmadge, U. Stroth, A. Kus, S. Murakami *et al.*, Nucl. Fusion **45**, 1684 (2005).
[3] Y. Idomura and M. Nakata, Phys. Plasmas **21**, 020706 (2014).
[4] J. Wesson and D.J. Campbell, *Tokamaks* (Oxford university press, 1997).
[5] K. Itoh, S.-I. Itoh and A. Fukuyama, *Transport and structural formation in plasmas* (Institute of Physics Pub, 1999).
[6] J.W. Connor and O.P. Pogutse, Plasma Phys. Control. Fusion **43**, 155 (2001).
[7] C.C. Petty, T.C. Luce, K.H. Burrell, S.C. Chiu, J.S. Degrassie, C.B. Forest, P. Gohil, C.M. Greenfield, R.J. Groebner, R.W. Harvey *et al.*, Phys. Plasmas **2**, 2342 (1995).
[8] X. Garbet, P. Mantica, C. Angioni, E. Asp, Y. Baranov, C. Bourdelle, R. Budny, F. Crisanti, G. Cordey, L. Garzotti *et al.*, Plasma Phys. Control. Fusion **46**, B557 (2004).
[9] S.J. Zweben, J.A. Boedo, O. Grulke, C. Hidalgo, B. LaBombard, R.J. Maqueda, P. Scarin and J.L. Terry, Plasma Phys. Control. Fusion **49**, S1 (2007).
[10] X. Garbet, Y. Idomura, L. Villard and T.H. Watanabe, Nucl. Fusion **50**, 043002 (2010).
[11] C.K. Kiefer, C. Angioni, G. Tardini, N. Bonanomi, B. Geiger, P. Mantica, T. Pütterich, E. Fable, P.A. Schneider, ASDEX Upgrade Team, EUROfusion MST1 Team and JET Contributors, Nucl. Fusion **61**, 066035 (2021).

[12] P.H. Diamond, C.J. McDevitt, Ö.D. Gürcan, T.S. Hahm, W.X. Wang, E.S. Yoon, I. Holod, Z. Lin, V. Naulin and R. Singh, Nucl. Fusion **49**, 045002 (2009).
[13] T.I. Tsujimura, T. Kobayashi, K. Tanaka, K. Ida, K. Nagaoka, M. Yoshinuma, I. Yamada, H. Funaba, R. Seki, S. Satake *et al.*, Phys. Plasmas **29**, 032504 (2022).
[14] K. Ida, Z. Shi, H.J. Sun, S. Inagaki, K. Kamiya, J.E. Rice, N. Tamura, P.H. Diamond, G. Dif-Pradalier, X.L. Zou *et al.*, Nucl. Fusion **55**, 013022 (2015).
[15] N. Tamura, S. Inagaki, K. Ida, T. Shimozuma, S. Kubo, T. Tokuzawa, K. Tanaka, S.V. Neudatchin, K. Itoh, D. Kalinina *et al.*, Phys. Plasmas **12**, 110705 (2005).
[16] X. Garbet, P. Mantica, F. Ryter, G. Cordey, F. Imbeaux, C. Sozzi, A. Manini, E. Asp, V. Parail, R. Wolf *et al.*, Plasma Phys. Control. Fusion **46**, 1351 (2004).
[17] P. Mantica, D. Strintzi, T. Tala, C. Giroud, T. Johnson, H. Leggate, E. Lerche, T. Loarer, A.G. Peeters, A. Salmi *et al.*, Phys. Rev. Lett. **102**, 175002 (2009).
[18] U. Stroth, L. Giannone, H.J. Hartfuss, ECH group *et al.*, Plasma Phys. Control. Fusion **38**, 611 (1996).
[19] TFR group and FOM ECRH Team, Nucl. Fusion **28**, 1995 (1988).
[20] K.W. Gentle, M.E. Austin, J.C. DeBoo, T.C. Luce and C.C. Petty, Phys. Plasmas **13**, 012311 (2006).
[21] S. Inagaki, T. Tokuzawa, N. Tamura, S.-I. Itoh, T. Kobayashi, K. Ida, T. Shimozuma, S. Kubo, K. Tanaka, T. Ido *et al.*, Nucl. Fusion **53**, 113006 (2013).
[22] M. Lesur, P.H. Diamond and Y. Kosuga, Phys. Plasmas **21**, 112307 (2014).
[23] Y. Kosuga, S.-I. Itoh, P.H. Diamond, K. Itoh and M. Lesur, Nucl. Fusion **57**, 072006 (2017).
[24] T.H. Dupree, Phys. Fluids **25**, 277 (1982).
[25] I.B. Bernstein, J.M. Greene and M.D. Kruskal, Phys. Rev. **108**, 546 (1957).
[26] T.H. Dupree, Phys. Fluids **15**, 334 (1972).
[27] P.W. Terry, P.H. Diamond and T.S. Hahm, Phys. Fluids B **2**, 2048 (1990).
[28] Y. Kosuga, P.H. Diamond, L. Wang, Ö.D. Gürcan and T.S. Hahm, Nucl. Fusion **53**, 043008 (2013).
[29] S.-I. Itoh and K. Itoh, Sci. Rep. **2**, 860 (2012).
[30] S.-I. Itoh and K. Itoh, Nucl. Fusion **53**, 073035 (2013).
[31] J.Y. Kim, Y. Kishimoto, W. Horton and T. Tajima, Phys. Plasmas **1**, 927 (1994).
[32] Y. Kishimoto, T. Tajima, W. Horton, M.J. LeBrun and J.Y. Kim, Phys. Plasmas **3**, 1289 (1996).
[33] M. Lesur, P.H. Diamond and Y. Kosuga, Plasma Phys. Control. Fusion **56**, 075005 (2014).
[34] K. Ida, T. Kobayashi, K. Itoh, M. Yoshinuma, T. Tokuzawa, T. Akiyama, C. Moon, H. Tsuchiya, S. Inagaki and S.-I. Itoh, Sci. Rep. **6**, 36217 (2016).
[35] K. Ida, T. Kobayashi, M. Yoshinuma, T. Akiyama, T. Tokuzawa, H. Tsuchiya, K. Itoh and S.-I. Itoh, Sci. Rep. **8**, 2804 (2018).
[36] K. Ida, T. Kobayashi, M. Yoshinuma, K. Nagaoka, K. Ogawa, T. Tokuzawa, H. Nuga and Y. Katoh, Communi. Phys. **5**, 228 (2022).
[37] T. Kobayashi, M. Yoshinuma, W. Hu and K. Ida, Phys. Plasmas **30**, 052303 (2023).
[38] K. Saeki, P. Michelsen, H.L. Pécseli and J.J. Rasmussen, Phys. Rev. Lett. **42**, 501 (1979).
[39] B. Lefebvre, L.-J. Chen, W. Gekelman, P. Kintner, J. Pickett, P. Pribyl, S. Vincena, F. Chiang and J. Judy, Phys. Rev. Lett. **105**, 115001 (2010).
[40] W. Fox, M. Porkolab, J. Egedal, N. Katz and A. Le, Phys. Rev. Lett. **101**, 255003 (2008).
[41] Y. Asahi, K. Fujii, D.M. Heim, S. Maeyama, X. Garbet, V. Grandgirard, Y. Sarazin, G. Dif-Pradalier, Y. Idomura and M. Yagi, Phys. Plasmas **28**, 012304 (2021).
[42] N. Kasuya, M. Nunami, K. Tanaka and M. Yagi, Nucl. Fusion **58**, 106033 (2018).
[43] S. Matsuoka, H. Sugama and Y. Idomura, Phys. Plasmas **28**, 064501 (2021).
[44] H. Funaba, R. Yasuhara, H. Uehara, I. Yamada, R. Sakamoto, M. Osakabe and D.J. Den Hartog, Sci. Rep. **12**, 1 (2022).
[45] P. Sprangle, E. Esarey and A. Ting, Phys. Rev. Lett. **64**, 2011 (1990).
[46] H.S. Fu, F. Chen, Z.Z. Chen, Y. Xu, Z. Wang, Y.Y. Liu, C.M. Liu, Y.V. Khotyaintsev, R.E. Ergun, B.L. Giles *et al.*, Phys. Rev. Lett. **124**, 095101 (2020).
[47] I.H. Hutchinson, Phys. Plasmas **24**, 055601 (2017).
[48] N. Kitamura, M. Kitahara, M. Shoji, Y. Miyoshi, H. Hasegawa, S. Nakamura, Y. Katoh, Y. Saito, S. Yokota, D.J. Gershman *et al.*, Science **361**, 1000 (2018).
[49] T. Tajima and J.M. Dawson, Phys. Rev. Lett. **43**, 267 (1979).